

## Emission of low-energy electrons from multicharged ions interacting with metal surfaces

P. A. Zeijlmans van Emmichoven\*

*Oak Ridge National Laboratory, Oak Ridge, Tennessee 37831-6372*

*and Joint Institute for Heavy Ion Research, Holifield Heavy Ion Research Facility, Oak Ridge, Tennessee 37831-6374*

C. C. Havener

*Oak Ridge National Laboratory, Oak Ridge, Tennessee 37831-6372*

I. G. Hughes

*Oak Ridge National Laboratory, Oak Ridge, Tennessee 37831-6372*

*and Joint Institute for Heavy Ion Research, Holifield Heavy Ion Research Facility, Oak Ridge, Tennessee 37831-6374*

D. M. Zehner and F. W. Meyer

*Oak Ridge National Laboratory, Oak Ridge, Tennessee 37831-6372*

(Received 3 August 1992; revised manuscript received 9 December 1992)

Low-energy electron spectra are reported for 60- and 100-keV multicharged ions interacting at an incident angle of  $20^\circ$  with Au and Cu surfaces. Analysis of the spectra indicate that at least two features contribute. The first feature represents the major contribution to the total electron yield and consists of 5–10-eV electrons emitted over a wide range of angles. The angular distribution of this component is not symmetric with respect to the surface normal, but shows an increase in the forward direction of the incident ions. It will be shown that this component arises predominantly from below the surface. Possible potential-emission mechanisms which may contribute will be discussed. The second feature, which constitutes a minor part of the overall electron emission, occurs at higher electron energies ( $\sim 20$  eV), and is peaked at the extreme forward angles. Binary encounters between incident ions and metal electrons at the surface-vacuum interface will be shown to describe the main features of this component. At even higher electron energies ( $> 40$  eV) the spectra show a tail whose slope does not depend on either the initial charge state or kinetic energy of the incident ions. The invariance with kinetic energy is in sharp contrast with the corresponding experimental results from ion-atom collisions.

PACS number(s): 79.20.Nc, 34.70.+e, 79.90.+b

### I. INTRODUCTION

During the interactions of slow multicharged ions ( $v_{\text{ion}} \simeq 0.1$  a.u.) with metal surfaces, electrons from the conduction band are captured into Rydberg levels of the ions at large distances above the surface, leading to the formation of multiexcited, so-called “hollow” atoms [1–14]. As they approach the surface, the deexcitation of these multiexcited atoms (with  $Z < 20$ ) presumably takes place via a cascade of intra-atomic Auger transitions, each step resulting in the emission of a low-energy electron [15]. The time the ions spend above the surface at these interaction energies, however, is much shorter than the estimated overall cascading time for complete relaxation [5,10]. Therefore it is likely that the atoms will be in a multiexcited state when they reach and interact with the surface. Close to the surface, the screening of the positive cores of the projectiles by the metal conduction electrons will increase rapidly, thereby strongly decreasing the binding energy of the excited projectile electrons, which will be either recaptured by the metal into unoccupied levels, promoted to the continuum, or “peeled off” [10] at impact. Subsequent electron capture very close to the surface and after the ions have penetrated the bulk will take place into much lower  $n$  states of the ions, fol-

lowed by rapid innershell intra-atomic Auger transitions [6].

For  $\text{N}^{6+}$  and  $\text{O}^{7+}$  ions grazing incident on metal surfaces, these intra-atomic Auger transitions filling the  $L$  shells and the  $K$  shell have been observed experimentally [4,5]. Recently, we have shown that the observed  $KLL$  Auger electron yields are consistent with model simulations which assume that capture into low- $n$  states occurs when the ions penetrate the surface, followed by inner-shell Auger transitions [6,16]. Above-surface  $KLL$  emission was shown to occur [6] only at very small perpendicular velocities ( $v_{\text{ion}} \leq 0.01$  a.u.), in which the effective time the ions spend above the surface approaches the overall cascading time. The intensity of the observed above-surface  $KLL$  emission is in reasonable agreement with the results from model simulations for the above-surface Auger cascade and can thus be argued to confirm the transient existence of these interesting atomic systems above metal surfaces. Direct experimental evidence for the production and relaxation of multiexcited “hollow” atoms above metal surfaces, however, has yet to be found. Also, the ultimate fate of the Rydberg electrons carried by such hollow atoms toward the surface (recapture by the surface, promotion into the continuum, or “peeling off” due to projectile core screening) remains an

incompletely resolved question. Recent statistical analysis of the electron emission for much lower projectile velocities, in concert with modeling studies [17], has suggested that these electrons may contribute to the overall yield via the mechanisms enumerated above, as well as via fast Auger processes [18].

The main focus of experiments to date has been on the characteristic *KLL* and *LMM* Auger transitions and, more recently, on *K* x-ray transitions [7–9]. The dominant contribution to the electron emission, however, consists of low-energy electrons. A study of these electrons should provide more detailed information on the atomic structure and deexcitation mechanisms of “hollow” atoms since, e.g., the initial phase of the above-mentioned cascade involves predominantly low-energy electrons arising in Auger transitions involving closely spaced Rydberg states. Information on these low-energy electrons can be obtained from total-electron-yield measurements [19], from emission-statistics measurements [18,20,21], and from low-energy electron spectra. The analysis of low-energy electrons, however, is complicated by contributions from, e.g., secondary electron emission induced by electrons traveling in the surface, and kinetic emission, which has been shown to contribute significantly for ion velocities larger than roughly 0.05 a.u. [19,22].

Presented here are the low-energy parts of the electron spectra measured for various *N* ions incident at 20° on Cu(001) and Au(011) single-crystal surfaces. Measurements have been performed for a series of observation angles, for several different ion velocities and charge states, and as a function of the surface cleanliness. The kinetic energy of the ions is in the range of 60–100 keV, which is sufficient for significant penetration of the bulk to occur under the incidence conditions used. An analysis of the low-energy electron spectra shows the presence of at least two components. The first has an energy distribution which peaks at energies below 10 eV and constitutes the major fraction of overall electron emission. The dependence of this component on the emission angle suggests that the bulk of these electrons is produced in the subsurface region. The second feature makes up only a small fraction of the total electron emission and consists of 15–20-eV electrons emitted at extreme forward angles. The latter feature is consistent with electron ejection in binary-encounter collisions between the incident ions and metal electrons at the surface-vacuum interface. In the region of electron energies  $\geq 40$  eV, the electron spectra are characterized by exponentially decreasing slopes, which are virtually invariant with the charge state and kinetic energy of the incident ions. The mechanisms that may be responsible for these various features in the electron spectra will be explored.

## II. EXPERIMENT

As the apparatus has been described elsewhere [2,16], only a brief description will be given here. The single-crystal surfaces of Cu(001) and Au(011) were prepared by cycles of sputter cleaning with 1-keV Ar<sup>+</sup> ions incident at an angle of approximately 30°, and annealing up to temperatures of 700°C. The surface cleanliness was fre-

quently checked by Auger electron spectroscopy (AES). The measurements were performed at a background pressure of typically  $10^{-8}$  Pa. Multicharged ions, extracted from the Oak Ridge National Laboratory Electron Cyclotron Resonance (ORNL-ECR) ion source, were directed on to the single-crystal surface. The crystal was mounted on a manipulator which allowed for a full rotation  $\Psi$  around an axis in the surface plane perpendicular to the incident ion beam, and for an azimuthal rotation  $\Phi$  of 90° around the surface normal. The angle-resolved electron energy spectra were measured with a hemispherical analyzer in combination with a channel plate detector. The analyzer was rotatable over about 120° in a plane containing the incident beam and the surface normal.

To ensure reliable detection of low-energy electrons, Helmholtz coils were used to minimize the magnetic field in the interaction region and the channel plate detector's front end was biased at +300 V to accelerate low-energy electrons before detection. Using the present setup, electrons with energies as low as 5 eV can be reliably detected. The spectra have an absolute uncertainty of roughly 30%, and a 10% relative uncertainty for successive spectra.

### A. Ion-induced electron emission from Cu(001)

The electron energy spectra measured at different observation angles are shown in Fig. 1 for 100-keV N<sup>6+</sup> ions. The spectra seem to consist of at least two components indicated by the vertical dashed lines, one having an energy distribution which peaks at energies below 10 eV, the other around 20 eV. The intensity of the sub-10-eV electrons strongly decreases for grazing observation angles. This suggests that the electron emission is dominated by emission from below the surface, where the number of electrons observed is limited by the path length that the electrons have to travel prior to escape from the surface. We will refer to these electrons as the

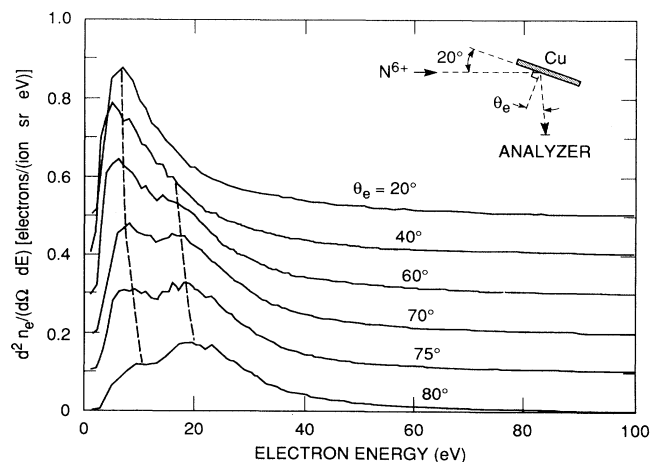


FIG. 1. Absolute electron energy spectra for 100-keV N<sup>6+</sup> ions incident on Cu(001) at 20° in the (100) plane. The results for six different observation angles are shown with offsets increasing in steps of 0.1 electrons/(ion sr eV). Two separate components (see text) are indicated by vertical dashed lines. The experimental setup is shown in the inset.

*subsurface* electrons. The intensity of the 20-eV electrons, on the other hand, strongly increases in the forward directions, indicating an emission mechanism that is both strongly correlated with the direction of the incident ions and located closer to the surface. We have made sure that these electrons originate from ion-surface interactions and not from, e.g., ion scattering in the analyzer, by applying a series of bias voltages to the crystal and observing the appropriate shifts of the electron energy distribution. We have also observed a dependence of the shape and position of this 20-eV component on the kinetic energy of the incident ions, as is shown in Fig. 2. Decreasing the kinetic energy of the incident ions from 100 to 60 keV results in a decrease of the width and total intensity of the peak and, also, a significant shift to lower energies of this peak from roughly 20 to 14.5 eV. Because of these "dynamic" properties, we will refer to electrons making up this peak as *dynamic* electrons. A discussion of possible emission mechanisms giving rise to these electrons is deferred to the next section.

It is interesting to study the high-energy tails of the electron energy distributions extending beyond the "dynamic" peak. The electron energy distributions for 60- and 100-keV  $N^{6+}$  ions incident at  $20^\circ$  on Cu(001) and for an observation angle of  $80^\circ$  with the surface normal are shown on a semilog plot in Fig. 3, together with the distributions for 68-keV  $N^{4+}$ , 34-keV  $N^{2+}$ , and 17-keV  $N^+$  ions for similar experimental conditions. It can be seen that the slope of the energy spectra at energies higher than 20 eV is virtually independent of both the kinetic energy *and* charge state of the incident ions. The slight increase in electron intensity observed in the 60-keV  $N^{6+}$  spectrum at energies around 80 eV and in the 68-keV  $N^{4+}$  spectrum at energies around 60 eV can be ascribed to *LMM* Auger electron emission from the moving projectiles [4,5]. The invariance of the slope with increasing kinetic energy of the incident ions is in sharp contrast to experimental observations [23] and theoretical under-

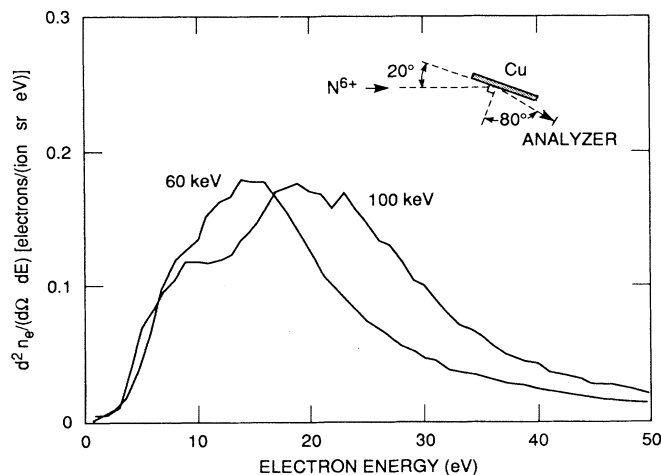


FIG. 2. Absolute electron energy spectra for 60- and 100-keV  $N^{6+}$  ions incident on Cu(001) at  $20^\circ$  in the (100) plane, observed at a forward angle of  $80^\circ$  with respect to the surface normal. The experimental setup is shown in the inset.

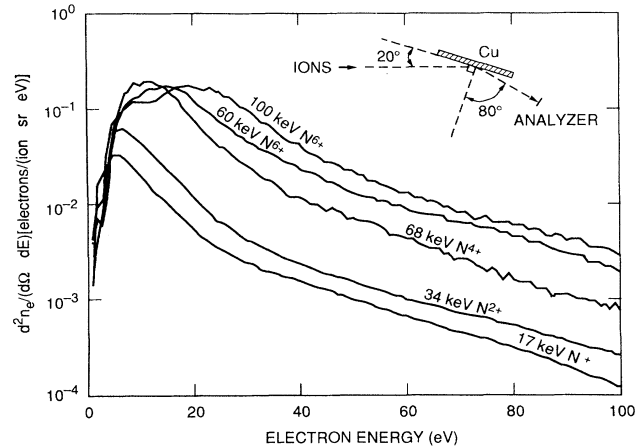


FIG. 3. Absolute electron energy distributions for 60- and 100-keV  $N^{6+}$ , 68-keV  $N^{4+}$ , 34-keV  $N^{2+}$ , and 17-keV  $N^+$  ions incident on Cu(001) at  $20^\circ$  in the (100) plane, observed at a forward angle of  $80^\circ$  with respect to the surface normal. Note that the vertical axis has a logarithmic scale. The experimental setup is shown in the inset.

standing [24] of continuum electrons in ion-atom collisions, where a decrease in slope is observed with increasing kinetic energy. An explanation for the observed constant slope in the electron spectra for different ion kinetic energies and charge states in ion-surface collisions has yet to be found.

It is illustrative to show the effect of surface cleanliness on the emission of the low-energy electrons. The electron energy distribution for 100-keV  $N^{6+}$  ions incident at  $20^\circ$  has been measured in the forward direction at an angle of  $80^\circ$  with the surface normal at different time intervals subsequent to cleaning the Cu single-crystal surface. As can be seen in Fig. 4, a low-energy contribution increases strongly with time after preparing the Cu surface. Such a

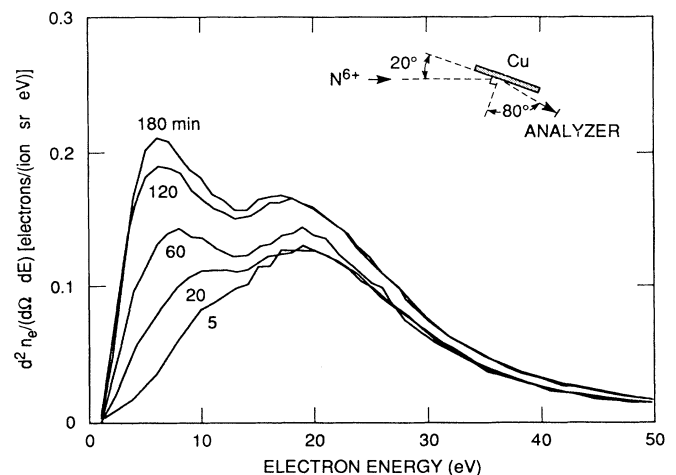


FIG. 4. Effect of surface cleanliness on the absolute electron energy distributions measured for 100-keV  $N^{6+}$  ions incident on Cu(001) at  $20^\circ$  in the (100) plane, observed at a forward angle of  $80^\circ$  with the surface normal. The time after completion of the sputter cleaning and annealing procedure is indicated in min. The experimental setup is shown in the inset.

strong increase suggests that the source of these electrons is located relatively close to the surface, so that the low-energy electrons can escape from the solid at such a grazing observation angle. By applying Auger electron spectroscopy, we have determined that after a few h the contamination of Cu mainly consists of low- $Z$  atoms like C, O, and N (N by implantation). Collisions between the projectiles and these low- $Z$  contaminants in the first few layers of the surface probably contribute to the observed strong increase of emission of "subsurface" electrons.

### B. Ion-induced electron emission from Au(011)

We have measured the ion-induced electron spectra for a Au(011) single-crystal surface for direct comparison with results obtained for Cu(001). The dependence on the observation angle of the electron energy distribution for 100-keV  $N^{6+}$  ions incident at  $20^\circ$  on Au(011) is shown in Fig. 5. The projection of the beam on the crystal surface is along the [100] direction. The two components observed for Cu(001) are also discernible in the energy spectra for Au(011), the first at energies below 10 eV with a broad angular distribution and the second at energies around 20 eV, which is strongly forward peaked. As for Cu(001), we will refer to the electrons making up these two components as the *subsurface* and *dynamic* electrons, respectively. The electron energy distributions for 60-, 85-, and 100-keV  $N^{6+}$  ions incident at  $20^\circ$  and for a forward observation angle of  $80^\circ$  with the surface normal are shown in Fig. 6. As can be seen in the figure, the energy distribution of the "dynamic" electrons has a similar dependence on the kinetic energy of the incident ions as was observed for Cu(001). The energy distribution of the

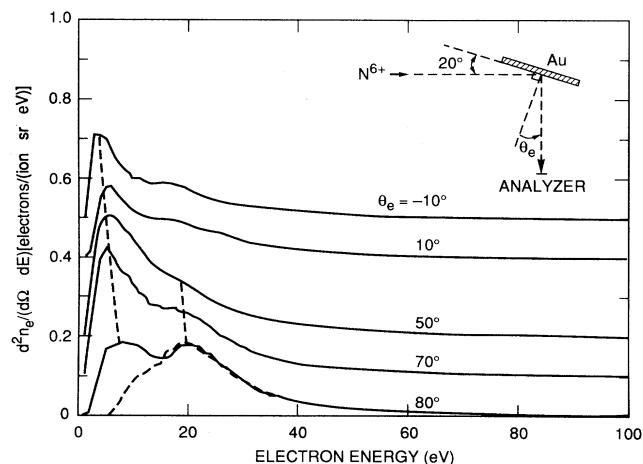


FIG. 5. Absolute electron energy distributions for 100-keV  $N^{6+}$  ions incident at  $20^\circ$  on Au(011). The projection of the incident beam on the crystal surface is along the [100] direction. The measurements shown are taken for five different observation angles. The offsets used are in tenths of electrons/(ion sr eV). The two components (see text) are indicated by vertical dashed lines. The experimental setup is shown in the inset. The dashed spectrum corresponds to the absolute electron energy distribution for Cu(001) taken for identical incidence conditions and an observation angle of  $80^\circ$  with the surface normal.

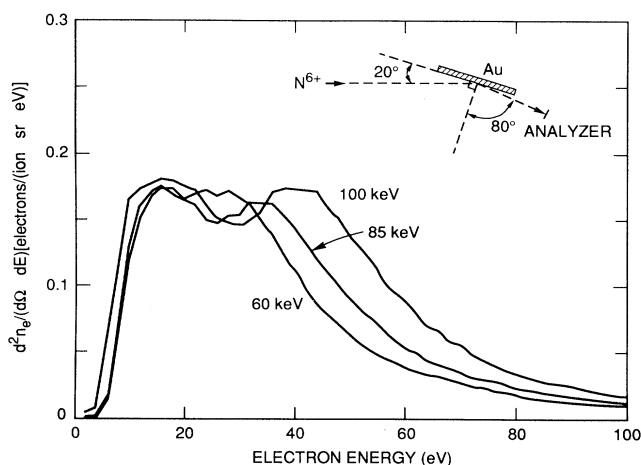


FIG. 6. Absolute electron energy spectra for 60-, 85-, and 100-keV  $N^{6+}$  ions incident on Au(011) at  $20^\circ$  observed at a forward angle of  $80^\circ$  with respect to the surface normal. The projection of the incident beam on the crystal surface is along the [100] direction. The experimental setup is shown in the inset.

"subsurface" electrons is roughly independent of the kinetic energy of the incident ions.

There is an additional structure in the Au spectra (see Fig. 5) appearing around 20 eV at close-to-normal observation angles that is not observed for Cu and which does not shift to higher energies as the kinetic energy of the ion is increased. In view of the latter, we feel this feature arises from a different mechanism than that ascribed the "dynamic" electrons. This component will not be discussed further in this paper.

The electron spectrum for Cu(001) taken for the most forward observation angle is indicated by the dashed line in Fig. 5. This direct comparison of the results obtained for Cu(001) and Au(011) shows that the contribution of "dynamic" electrons to the electron emission at this observation angle is virtually the same for both single-crystal surfaces (a similarity which is partly fortuitous considering the absolute uncertainty of the experiments), whereas the contribution of "subsurface" electrons is strikingly much larger in the case of Au(011). In addition, the sensitivity of the low-energy emission with respect to the elapsed time after cleaning the surface was not found for Au(011) as was observed for Cu(001) and shown in Fig. 4. Indeed, as we have observed with our Auger electron spectroscopy diagnostics, the Au surface remains cleaner for a significantly longer time than Cu.

It is interesting to measure the low-energy electron emission as a function of the orientation of the crystal with respect to the incident beam direction. The "subsurface" electrons for Au(011) exhibit an intensity variation of roughly 20–30% with azimuthal orientation angle, confirming that the emission takes place from below the surface. Typical results for two azimuthal angles are shown in Fig. 7, one obtained close to a maximum, the other close to a minimum of the "subsurface" intensity. The measurements were taken for similar incidence conditions as those shown in Fig. 5, and for a forward obser-

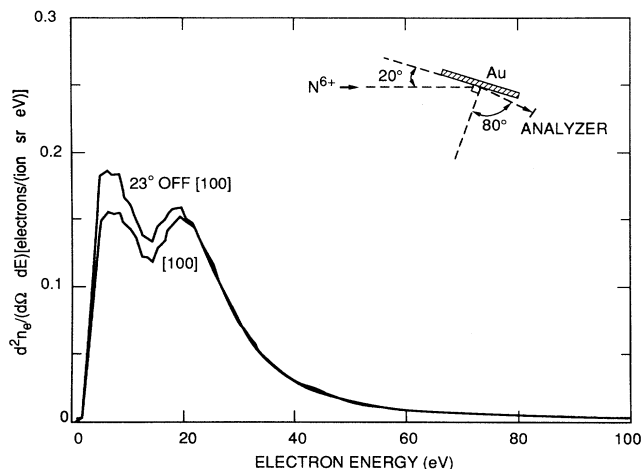


FIG. 7. Absolute electron energy distributions for 100-keV  $N^{6+}$  ions incident on Au(011) at  $20^\circ$  observed at a forward angle of  $80^\circ$  with respect to the surface normal for two different azimuthal orientation angles. The projection of the incident beam on the crystal surface is along the [100] direction in one case,  $23^\circ$  off this axis in the second case. The experimental setup is shown in the inset.

vation angle of  $80^\circ$  with the surface normal. Note that the intensity of “dynamic” electrons shows virtually no dependence on the azimuthal orientation angle, which indicates that these electrons originate closer to the surface.

The dependence of the electron energy distribution on the charge state of the incident ions is illustrated in Fig. 8 for 6.1-keV/amu  $N^{6+}$ ,  $N^{5+}$ , and  $O^{6+}$  ions incident at  $20^\circ$  on Au(011) for an observation angle of  $80^\circ$  with the surface normal. Both the energy distribution and intensity of the “subsurface” electrons for heliumlike  $N^{5+}$  and  $O^{6+}$  ions are virtually identical. In contrast, the “subsurface” energy distribution for hydrogenlike  $N^{6+}$  appears to have shifted to higher energies. This behavior suggests that the detailed energy distribution of “subsurface” electrons emitted in a forward direction may depend on the presence of a  $K$ -shell vacancy, which would be consistent with the known survival of the  $K$ -shell vacancies [6] beyond the surface-vacuum interface.

We next address the dependence of the “dynamic” component on the presence of a  $K$ -shell vacancy in the incident ion. Figure 8 also shows the presence of the “dynamic” component for heliumlike  $N^{5+}$  and  $O^{6+}$  ions. The intensity of the “dynamic” component for these heliumlike ions is estimated to be at least 50% of the corresponding intensity for the hydrogenlike  $N^{6+}$ . This indicates that the emission of “dynamic” electrons for heliumlike ions cannot be explained by the small fraction of hydrogenlike metastables (about 6% for  $N^{5+}$  and 2.5% for  $O^{6+}$  [25]) in the incident ion beams. Such a large “dynamic” component for heliumlike ions indicates that the presence of a  $K$ -shell vacancy is not necessary for the emission of these “dynamic” electrons. In Fig. 8 we have plotted as the dashed curve the hydrogenlike spectrum scaled down by a factor of 0.74. This shows that even the energy distribution of “dynamic” electrons is not significantly affected by the presence of a  $K$ -shell vacan-

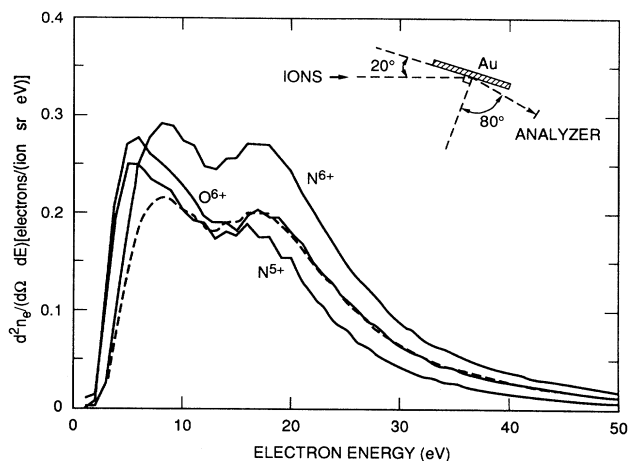


FIG. 8. Absolute electron energy distributions for 6.1-keV/amu  $N^{6+}$ ,  $N^{5+}$ , and  $O^{6+}$  ions incident on Au(011) at  $20^\circ$  observed at a forward angle of  $80^\circ$  with respect to the surface normal. The projection of the incident beam on the crystal surface is along the [100] direction. The dashed spectrum shows the  $N^{6+}$  spectrum scaled down by a factor of 0.74. The experimental setup is shown in the inset.

cy. Note, however, that the “dynamic” component for  $N^{5+}$ , when compared to the component for  $N^{6+}$  or  $O^{6+}$ , appears to have shifted slightly towards lower energies. This suggests a weak dependence on the charge state of the incident ions.

### III. DISCUSSION

We first present a quantitative deconvolution analysis of the contributions to the total electron yield of the observed *subsurface* electrons at very low energies and *dynamic* electrons at slightly higher energies. We will then discuss possible emission mechanisms for “subsurface” and “dynamic” electrons.

#### A. Contributions of “subsurface” and “dynamic” electrons

We performed an analysis on the spectra shown in Fig. 1 obtained for 100-keV  $N^{6+}$  ions incident at  $20^\circ$  on Cu(001). The results are shown as a polar plot in Fig. 9, in which the measured energy-integrated electron emission is shown as a solid line (labeled “experiment”). In order to deconvolute the “subsurface” and “dynamic” components, we started by assuming that the electron energy distribution measured at an observation angle of  $20^\circ$  relative to the surface normal is dominated by emission of “subsurface” electrons. To estimate the contribution of “subsurface” electrons at more forward emission angles, the latter distribution was appropriately scaled to match the “subsurface” peak heights of the spectra measured at more forward emission angles. The “dynamic” components were then obtained from the subtracted spectra.

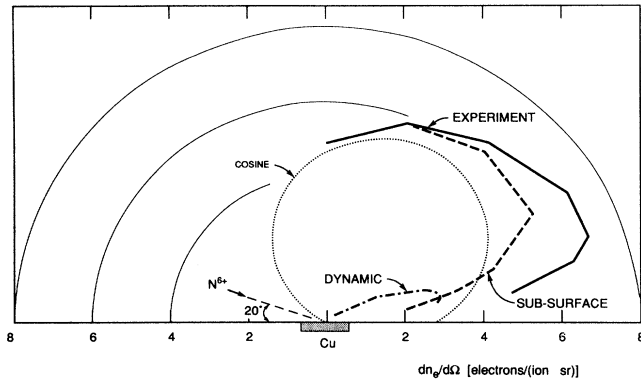


FIG. 9. Polar plot of the angular dependence of the energy-integrated electron emission for 100-keV  $N^{6+}$ -Cu(001) collisions. The ion beam is incident at  $20^\circ$  in the (100) plane. The energy-integrated electron emission in a specific direction corresponds to the distance from the origin (center of the crystal). Contours of constant electron emission are indicated by thin solid lines. The measured energy-integrated electron emission is indicated by the solid line, which is decomposed in the "subsurface" contribution (dashed line) and the "dynamic" contribution (dashed-dotted line). The dotted line shows a cosine distribution which is slightly tilted in the forward direction.

The estimated contributions of "subsurface" and "dynamic" electron emission thus obtained are indicated in Fig. 9 by dashed and dashed-dotted lines, respectively. Figure 9 clearly shows that the "subsurface" electrons constitute the dominant part of the total electron emission for most emission angles, whereas the "dynamic" electrons contribute only at large forward angles. The angular distribution of the "subsurface" component is *not* symmetric about the surface normal but has larger intensities for angles in the forward direction (up to angles of about  $60^\circ$  with the normal). This implies that at least one contributing mechanism gives rise to preferential emission of electrons in the forward direction. This "subsurface" contribution somewhat resembles a cosine distribution (dotted line in Fig. 9) about an axis tilted forward by  $30^\circ$  with respect to the surface normal. Assuming symmetry of emission about this axis, an estimate of the "subsurface" contribution to the total electron yield of approximately 20 electrons per incident ion is obtained. For the "dynamic" component we assume cylindrical symmetry about an axis in the direction of maximum intensity. This leads to the assumption that the emission of "dynamic" electrons is confined to a spatial angle of only a few tenths of a sr, corresponding to an integrated contribution to the total electron yield of roughly 0.5 to 1 electrons per incident ion. The sum of the "subsurface" and "dynamic" contributions yields an estimate for the total electron yield of roughly 21 electrons per ion. This number is in reasonable agreement with the measured total electron yield of  $17 \pm 3$  electrons per ion determined from independent measurements of biased and unbiased target currents (for the experimental procedure see [5]).

It is important to note that the contribution of "subsurface" electrons to the electron emission for clean

Cu(001) strongly decreases for grazing observation angles. The observed strong decrease for clean Cu(001) suggests that the electrons originate from well below the surface so that the path lengths prior to escape from the surface are comparable to the inelastic mean free path. For "dirty" Cu(001) and clean Au(011), on the other hand, significant emission of "subsurface" electrons is observed even for these grazing observation angles with the surface, suggesting emission within the first few layers of the crystal surface as well. Additional measurements performed at these grazing observation angles may provide important information on the electron ejection mechanisms active in the first few layers of the target surface.

### B. Emission of "subsurface" electrons

The experimental observations suggest that for our experimental conditions of relatively high ion energies and rather large angles of incidence, the major part of multicharged ion-induced electron emission consists of electrons which originate in the subsurface region. These "subsurface" electrons are emitted over a wide angular range, whose dependence resembles a cosine distribution around an axis tilted forward with respect to the surface normal.

Cosine distributions describing the angular dependence of electron emission from *low-charge-state* ion-metal surface interactions have been previously observed [26], and are explicable within the following simple model for subsurface emission. We assume that the kinetic energy and angle of incidence of the ions are sufficient to give rise to significant penetration in the bulk when compared to the inelastic mean free path for low-energy electrons (30–40 a.u. for 10-eV electrons [27]). The measured angular distribution of emitted electrons will then be determined by both the directly escaping electrons and the secondary electrons arising from the complex electron collision cascade. The effect of the inelastic mean free path on the escape probability of directly emitted electrons can be taken into account by a simple exponential function:

$$P_e(\theta_e) = \exp[-d/(\lambda \cos \theta_e)], \quad (1)$$

with  $P_e(\theta_e)$  the escape probability of an electron emitted at an angle  $\theta_e$  with the surface normal,  $d$  the depth below the surface at which the electron originates, and  $\lambda$  the inelastic mean free path of the electron. Assuming that the production of electrons takes place uniformly and isotropically in a slab with a thickness large compared to the inelastic mean free path, and integrating the escape probability  $P_e(\theta_e)$  over the depth  $d$  at which the electrons originate, yields a cosine distribution around the surface *normal* for the average escape probability for directly escaping electrons. Similar arguments hold for the average escape probability for the secondary electrons arising from the complex collision cascade. The angular distribution of emitted electrons will reflect this cosine distribution, since it is a direct reflection of the average escape probability.

The observed angular distribution of electron emission

from *highly charged* ion–Cu(001) interactions can be understood in part using the above model. For the ion energies considered here, the penetration depth of the ions is large compared with the inelastic mean free path. We ascribe the main features of the observed angular distribution shown in Fig. 9 to the effect of the inelastic mean free path on the escape probability of electrons produced rather deep in the solid. As outlined above for low-charge-state ions, this leads to a cosine distribution in the electron emission. The observed forward tilt of the cosine distribution is caused by an additional component exhibiting preferential emission in the forward direction. Possibilities for such emission mechanisms are discussed below.

When the  $N^{6+}$  ions penetrate the surface, the screening of the ions by metal electrons results in a strong decrease of the binding energy of ionic energy levels. This sudden screening will result in any Rydberg electrons captured above the surface becoming unbound and “peeled” off. The electrons that are emitted have an initial velocity component in the direction of the incident ion, which, especially for these high incident velocities, could result in emission in the forward direction. In addition to the “peeling” off of the Rydberg electrons, metal electrons will be captured by the ions into low-lying  $n$  levels like the  $M$  shell [16] and, in later stages of neutralization, possibly even the  $L$  shell. Deexcitation of these *excited* atoms most likely takes place via Auger-type mechanisms in which projectile and/or metal electrons are involved. If the emission consists predominantly of projectile electrons or metal electrons which are subsequently post-accelerated by the projectile, a preferential emission in forward angles is likely. By whatever mechanism forward emission is created, it will not be “washed out” by subsequent inelastic collisions if it takes place relatively close to the surface. Kinetic emission taking place in the first few layers may, of course, also contribute to the enhanced emission in forward angles.

We ascribe the intensity of “subsurface” electrons observed for Au(011) in the forward direction (see Fig. 5) to the production of electrons within the first few layers of the crystal where the escape probability even for these grazing observation angles is relatively high. That these low-energy electrons are emitted from below the surface is consistent with the azimuthal variation of the measured intensity, as is shown in Fig. 7. The energy distribution of these “subsurface” electrons does not depend critically on the kinetic energy of the incident ions, as is shown in Fig. 6. A slight dependence of the electron energy distribution on the initial presence of a  $K$ -shell vacancy has been observed (Fig. 8).

It is interesting to note the difference in intensity of this observed “subsurface” component between Cu(001) and Au(011) as is shown in Fig. 5. One of the possible contributions to “subsurface” electron emission, as discussed above, is from Auger decay of excited atoms in the first few layers of the surface. If electrons from the conduction band are involved in these Auger processes, differences in the surface density of states (SDOS) of Cu and Au would give rise to differences in the resulting electron energy distributions. The SDOS of Cu has a

large density of electrons at an energy of about 2–4 eV below the Fermi energy, whereas for Au the SDOS consists of a significant density at binding energies ranging from about 2–7 eV below the Fermi energy [28]. Since the work functions of the two metals are approximately equal [29], Auger transitions may give rise to emission of lower-energy electrons for Au(011) than for Cu(001) due to larger initial binding energies of the metal electrons involved. Such interatomic Auger electrons may explain the enhancement of the low-energy “subsurface” component observed for Au(011) for forward grazing observation angles. For Cu(001) this would imply contributions of interatomic Auger electrons at higher electron energies, where they cannot be distinguished from the “dynamic” electrons.

There may be additional mechanisms that result in low-energy electron emission and are therefore included in the “subsurface” component of Fig. 9 but do not occur below the surface. One such mechanism is the promotion to the continuum of excited atomic electrons. The binding energy of excited atomic electrons captured at large distances above the surface decreases with decreasing projectile-surface distance due to an increase of screening of the projectile ion core as a result of the autoionization cascade and/or the image charge interaction. The excited electrons will, when their binding energy becomes less than the work function, eventually be either recaptured by the metal surface or promoted to the continuum. Extensive theoretical calculations for our experimental conditions (i.e., non-normal incidence) have not been performed to date, although recent related work is available for faster ions [30]. In the case of promotion to the continuum, an angular distribution of emitted electrons peaked in the direction of the incident ions may be expected. A strongly peaked angular distribution, such as that observed for the “dynamic” electrons, however, seems unlikely. Preliminary calculations of promotion to the continuum due to the image charge interaction have been performed recently [31]. The calculated energy distribution consists of a peak at low electron energies with an exponential tail towards higher energies. The position of the peak was found not to depend on the kinetic energy of the incident ions, and the slope of the exponential tail was found to decrease significantly with increasing ion kinetic energy. These calculations are thus in marked contrast to the experimental observations shown in Fig. 3, i.e., an exponential tail whose slope is independent of the kinetic energy. We therefore conclude that promotion of excited atomic electrons may contribute to the total electron emission, but this contribution is, in general, “buried” in the low-energy part of the electron energy spectra. In addition, as previously discussed, any electrons remaining in Rydberg levels of the projectile may be “peeled off” as the projectiles penetrate the metal surface due to the sudden increase of screening of the projectile core.

### C. Emission of “dynamic” electrons

We have estimated that the “dynamic” electrons contribute roughly 0.5–1 electrons per incident ion to the to-

tal electron yield. The dependence of the energy distribution of the “dynamic” electrons on the kinetic energy of the incident ions is shown in Figs. 2 and 6 for Cu(001) and Au(011), respectively. In summary, an increase of the kinetic energy of the incident ions results in a broadening and a strong shift to higher energies of the energy distribution, in addition to an increase of the total intensity. These results suggest that the production mechanisms for “dynamic” electrons become more efficient with increasing kinetic energy of the incident ions, thus excluding mechanisms which require long interaction times such as Auger cascading *above* the surface. The observed independence of the energy distribution and intensity of the “dynamic” electrons on the target material (Fig. 5), on the cleanliness of the surface (Fig. 4), and on the azimuthal orientation angle of the single-crystal surface (Fig. 7) suggest production very close to the *surface-vacuum interface*. This is confirmed in the fact that most of the “dynamic” electrons are observed to be emitted into extreme forward angles (see Figs. 1, 5, and 9), where escape from any significant depth below the surface would be attenuated. One mechanism that may result in the emission of low-energy electrons very close to the surface-vacuum interface is binary-encounter collisions between incident ions and metal electrons.

Emission of electrons can occur as a result of such binary-encounter collisions between the incident ion and electrons from the conduction band at the surface-vacuum interface [30]. This binary-encounter mechanism is well known in MeV ion-atom collisions [32], where it appears as a distinct feature in the electron energy spectra in extreme forward directions, at energies close to four times the equivalent electron energy of the ions [32], and with a width determined by the initial momentum distribution of the target electrons involved. In ion-surface collisions the momentum distribution of the target electrons is related to the SDOS. For 100-keV N ions the equivalent electron energy of about 4 eV is somewhat *smaller* than the Fermi energy of roughly 5.5 eV for Au and 7 eV for Cu [29]. This would result in a relatively broad electron energy distribution that may extend to very low electron energies. The maximum possible energy of binary-encounter electrons occurs for emission in the direction of the incident ions, i.e., towards the surface at a velocity which would correspond to the sum of twice the velocity of the incident ions and the Fermi velocity minus a correction for the initial potential energy of the metal electrons. Assuming an initial potential energy of the metal electrons of  $-10$  eV with respect to the vacuum level, we may expect electron energies in a range from 0 to 30–35 eV. The energy distribution of “dynamic” electrons measured at  $30^\circ$  with the incident ion beam ( $80^\circ$  with the surface normal, see Figs. 1 and 5) is confined within this estimated energy region for binary-encounter electrons. The measured energy distributions, then, may consist of these binary-encounter electrons emitted in the direction of the ions and subsequently scattered from the surface (binary-encounter electrons emitted directly at an angle of  $30^\circ$  with the incident ions may also contribute). The observed shift to lower energies of the energy distri-

bution of the “dynamic” electrons upon a decrease of the ion energy (see Figs. 2 and 6) is also consistent with an explanation in terms of emission of binary-encounter electrons. The shape of the resulting electron energy distribution is determined by the SDOS, by the dependence of the emission cross section on the initial kinetic energy of the electrons, and by the elastic- and inelastic-scattering cross sections for electrons from the solid surface. Note that the energy distributions of “dynamic” electrons for Cu(001) and Au(011) are virtually identical, indicating a weak dependence on the SDOS. A thorough theoretical treatment of this mechanism for multicharged ions very close to metal surfaces is needed. In fact, the validity of the binary-encounter approximation in our regime of ion energies and for ions at metal surfaces has yet to be investigated in detail.

The contribution of these electrons emitted very close to the surface is only a small fraction of the total electron yield (see Fig. 9). However, the interaction of ions with metal electrons below the surface may give rise to binary-encounter electrons along its entire trajectory. These electrons may contribute significantly to the total electron yield and could indeed constitute a significant component of *kinetic* emission.

#### IV. CONCLUDING REMARKS

The low-energy part of the electron spectra obtained in 60- and 100-keV multicharged ion-metal surface interactions at large angles of incidence is comprised of two distinct features. The first feature consists of very-low-energy electrons which are predominantly emitted from below the surface and constitute the dominant part of the total electron emission. Although the analysis of these “subsurface” electrons is complicated due to many possible contributing mechanisms, certain features were observed. For example, it was found that the presence of a *K*-shell vacancy resulted in a shift to higher energies in the energy distribution. Also, a strong sensitivity on the target material and cleanliness of the surface has been found. Further experimental studies are in progress to understand the different contributing mechanisms.

The second feature consists of electrons presumably emitted at the surface-vacuum interface which constitute a small contribution to the overall electron emission. We have shown that the emission of these electrons, which have been labeled “dynamic” electrons, is consistent with binary-encounter mechanisms between incident ions and metal electrons at the surface. Theoretical investigations of this interesting “kinetic” phenomenon are needed.

Finally, we have found that the slope of the exponential high-energy tail in the electron spectrum does not depend on the kinetic energy and charge state of the incident ions. No explanation for this independence is known.

#### ACKNOWLEDGMENTS

We are indebted to J. Burgdörfer, S. Yu. Ovchinnikov, and U. Thumm for stimulating discussions, S. H. Over-

bury and M. T. Robinson for providing guidance in running the MARLOWE simulation code and interpreting its results, and J. Hale and G. Ownby for their skilled technical assistance. This work was supported by the Office of Basic Energy Sciences, Division of Chemical Sciences

and the Office of Fusion Energy, U.S. Department of Energy, under Contract No. DE-AC05-84OR21400 with Martin Marietta Energy Systems, Inc., and the Joint Institute for Heavy Ion Research through Contract No. DE-FG05-87ER40361 with the University of Tennessee.

\*Present address: Departamento de Física de Materiales, Apdo. 1072, Universidad del País Vasco, 20080 San Sebastián, Spain.

- [1] S. T. de Zwart, A. G. Drentje, A. L. Boers, and R. Morgenstern, *Surf. Sci.* **217**, 298 (1989).
- [2] F. W. Meyer, C. C. Havener, S. H. Overbury, K. J. Reed, K. J. Snowdon, and D. M. Zehner, *J. Phys. (Paris) Colloq.* **50**, C1-263 (1989).
- [3] C. C. Havener, K. J. Reed, K. J. Snowdon, N. Stolterfoht, D. M. Zehner, and F. W. Meyer, *Surf. Sci.* **216**, L357 (1989).
- [4] L. Folkerts and R. Morgenstern, *Europhys. Lett.* **13**, 377 (1990).
- [5] P. A. Zeijlmans van Emmichoven, C. C. Havener, and F. W. Meyer, *Phys. Rev. A* **43**, 1405 (1991).
- [6] F. W. Meyer, S. H. Overbury, C. C. Havener, P. A. Zeijlmans van Emmichoven, and D. M. Zehner, *Phys. Rev. Lett.* **67**, 723 (1991).
- [7] J. P. Briand, L. de Billy, P. Charles, S. Essabaa, P. Briand, R. Geller, J. P. Desclaux, S. Bliman, and C. Ristori, *Phys. Rev. Lett.* **65**, 159 (1990).
- [8] H. J. Andrä, A. Simionovici, T. Lamy, A. Brenac, G. Lamboley, J. J. Bonnet, A. Fleury, M. Bonnefoy, M. Chassevent, S. Andriamonje, and A. Pesnelle, *Z. Phys. D* **21**, 5135 (1991).
- [9] M. Schulz, C. L. Cocke, S. Hagmann, M. Stöckli, and H. Schmidt-Bocking, *Phys. Rev. A* **44**, 1653 (1991).
- [10] J. Burgdörfer, P. Lerner, and F. W. Meyer, *Phys. Rev. A* **44**, 5674 (1991).
- [11] J. N. Bardsley and B. M. Penetrante, *Comm. At. Mol. Phys.* **27**, 43 (1991).
- [12] J. W. McDonald, D. Schneider, M. W. Clark, and D. Dewitt, *Phys. Rev. Lett.* **68**, 2297 (1992).
- [13] N. Vaecq and J. E. Hansen, *J. Phys. B* **24**, L469 (1991).
- [14] R. Köhrbrück, D. Lecler, F. Fremont, P. Roncin, K. Sommer, T. J. M. Zouros, J. Bleck-Neuhaus, and N. Stolterfoht, *Nucl. Instrum. Methods B* **56**, 219 (1991).
- [15] U. A. Arifov, L. M. Kishinevskii, E. S. Mukhamadiev, and E. S. Parilis, *Zh. Tekh. Fiz.* **43**, 181 (1973) [*Sov. Phys. Tech. Phys.* **18**, 118 (1973)].
- [16] F. W. Meyer, S. H. Overbury, C. C. Havener, P. A. Zeijlmans van Emmichoven, J. Burgdörfer, and D. M. Zehner, *Phys. Rev. A* **44**, 7214 (1991).
- [17] F. Aumayr, H. Kurz, and K. Töglhofer, in *Proceedings of the VIth International Conference on the Physics of Highly Charged Ions, September, 1992*, edited by P. Richard, M. Stöckli, L. Koch, and C. D. Lin (AIP, New York, in press).
- [18] H. Kurz, K. Töglhofer, H. Winter, and F. Aumayr, *Phys. Rev. Lett.* **69**, 1140 (1992).
- [19] M. Fehring, M. Delaunay, R. Geller, P. Varga, and H. Winter, *Nucl. Instrum. Methods B* **23**, 245 (1987).
- [20] G. Lakits, F. Aumayr, and H. Winter, in *Proceedings of the International Conference on the Physics of Multicharged Ions, Grenoble, France, Sept. 12–16, 1988* [*J. Phys. (Paris) Colloq.* **50**, C1-19 (1989)].
- [21] H. Winter, *Z. Phys. D* **21**, 129 (1991).
- [22] M. Delaunay, M. Fehring, R. Geller, D. Hitz, P. Varga, and H. Winter, *Phys. Rev. B* **35**, 4232 (1987).
- [23] P. H. Woerlee, Yu. S. Gordeev, H. de Waard, and F. W. Saris, *J. Phys. B* **14**, 527 (1981).
- [24] S. Yu. Ovchinnikov and E. A. Solov'ev, *Zh. Eksp. Teor. Fiz.* **91**, 477 (1986) [*Sov. Phys. JETP* **64**, 280 (1986)].
- [25] K. J. Snowdon, C. C. Havener, F. W. Meyer, S. H. Overbury, and D. M. Zehner, *Rev. Sci. Instrum.* **59**, 902 (1988).
- [26] K. H. Krebs, *Fortschr. Phys.* **16**, 419 (1968).
- [27] L. C. Feldman and J. W. Mayer, *Fundamentals of Surface and Thin Film Analysis* (Elsevier, New York, 1986), p. 129.
- [28] J. C. Fuggle, L. M. Watson, D. J. Fabian, and P. R. Norris, *Solid State Commun.* **13**, 507 (1973).
- [29] N. W. Ashcroft and N. D. Mermin, *Solid State Physics* (Holt, Rinehart and Winston, New York, 1981), p. 364.
- [30] Uwe Thumm, *J. Phys. B* **25**, 421 (1992).
- [31] S. Y. Ovchinnikov and J. Macek, in *Proceedings of the VIth International Conference on the Physics of Highly Charged Ions, September, 1992* (Ref. [17]).
- [32] D. R. Schultz and R. E. Olson, *J. Phys. B* **24**, 3409 (1991).